Author Manuscript

Author Manuscript

Author Manuscript

Author Manuscript

HHS Public Access

Author manuscript

FASEB J. Author manuscript; available in PMC 2021 January 04.

Published in final edited form as:

FASEB J. 2020 February ; 34(2): 2376–2391. doi:10.1096/fj.201901791R.

Periovulatory insulin signaling is essential for ovulation, granulosa cell differentiation, and female fertility

Nikola Sekulovski, **Allison E. Whorton**, **Mingxin Shi**, **Kanako Hayashi**, **James A. MacLean II**

Department of Physiology, Southern Illinois University School of Medicine, Life Science III, 1135 Lincoln Drive, Carbondale, IL 62901-4306

Abstract

Recent studies have demonstrated an essential role for insulin signaling in folliculogenesis as conditional ablation of *Igf1r* in primary follicles elicits defective FSH responsiveness blocking development at the preantral stage. Thus the potential role of insulin action in the periovulatory window and in the corpus luteum is unknown. To examine this, we generated conditional *Insr*, I*gf1r*, and double receptor knockout mice driven by *Pgr-Cre*. These models escape the preantral follicle block and in response to superovulatory gonadotropins exhibit normal distribution of ovarian follicles and corpora lutea. However, single ablation of *Igf1r* leads to subfertility and mice lacking both receptors are infertile. Double knockout mice have impaired oocyte development and ovulation. While some oocytes are released and fertilized, subsequent embryo development is retarded, and the embryos potentially fail to thrive due to lack of luteal support. In support of this, we found reduced expression of key enzymes in the steroid synthesis pathway and reduced serum progesterone. In addition to metabolic and steroidogenic pathways, RNA sequencing analysis revealed TCF3 as an important transcription factor downstream of insulin signaling. Collectively, these results highlight the importance of growth factors of the insulin family during two distinct windows of follicular development, ovulation and lutenization.

Keywords

Insulin signaling; Female reproduction; Ovary; Knockout mouse

Introduction

Insulin and the highly related insulin-like growth factors 1 and 2 (IGF1 and IGF2) govern a wide variety of physiological processes related to metabolism, cell proliferation and development, and cell survival (1). These growth factors act by signaling through membrane-associated tyrosine kinase receptors including the insulin receptor (INSR) and the IGF1 receptor (IGF1R) and in some instances hybrid receptors containing subunits from both INSR and IGF1R (2, 3). Insulin and IGF1 ligands will preferentially bind to their own

Corresponding Author: James A. MacLean II, Ph.D., Department of Physiology, Southern Illinois University, Life Science III, Room 2071, 1135 Lincoln Drive, Carbondale, IL 62901-4306, 618-453-1579 (Office), jmaclean@siumed.edu.

Author Contributions. N. Sekulovski, K. Hayashi, and J. MacLean designed the study; N. Sekulovski, A. Whorton, M. Shi, and J. MacLean performed research. N. Sekulovski and J. MacLean analyzed data and wrote the manuscript.

Disclosure: The authors have no financial interests to disclose.

Author Manuscript Author Manuscript Author Manuscript Author Manuscript

receptors, but both ligands can bind with reduced affinity and activate downstream signaling cascades (4). In addition to the primary ligands, placental mammals have 6 active IGF binding proteins that modulate insulin hormone stability, insulin receptor activity, and perform IGF-independent actions that add complexity to functional assessment of the IGF/IGFBP axis (5). The consequences of disruption of insulin signaling in vitro and in vivo, either by ligand ablation, receptor ablation, or disruption via biochemical agents in many tissues and cell types, including the ovary has recently been reviewed (6). The relative contribution of ligand/receptor combinations to perform conserved functions is variable by both tissue and species. For example, stimulation of ovarian granulosa cells by follicle stimulating hormone (FSH) is dependent upon IGF1R activation, but in rodents IGF1 stimulates the receptor, whereas human granulosa cells respond specifically via IGF2 (7, 8). Regardless of ligand, activation of INSR and IGF1R initiates a conserved cascade of phosphorylation events mediated by the Ras-MAPK and AKT/PI3K pathways (1, 6). Thus, the in vivo action of insulin signaling may be better examined by ablation of the receptors rather than combinations of ligand and binding protein mutations.

Mouse insulin receptor knockout studies aimed at assessing the role of insulin signaling in ovarian function have been hindered by growth defects and lethality following complete INSR or IGF1R receptor ablation (9-11). While insulin receptors are present in the oocyte, single and double ablation of *Insr* and *Igf1r* genes conditionally in oocytes, results in normal oocyte development, maturation, fertilization, and live births (12). Dual ablation of INSR/IGF1R specifically in the embryonic gonad causes sex reversal and disrupts ovarian development (13), precluding use of that model to examine folliculogenesis and ovulation. Folliculogenesis begins when the oocyte, arrested in prophase I of meiosis, surrounded by a single layer of granulosa cells is activated and undergoes rapid growth and differentiation to give rise sequentially to primary, secondary, preantral, antral, and ultimately preovulatory follicles that are capable of releasing their mature oocytes in the context of proper hormone-mediated inflammatory rupture (14, 15). In vitro studies had previously established a role for IGF1 signaling in FSH-dependent granulosa cell growth and differentiation, hormone production, and acquisition of luteinizing hormone (LH) responsiveness (7, 16-18). Recently, conditional ablation of *Igf1r* signaling in granulosa cells using a combination of two Cre drivers (*Esr2* and *Cyp19*) was employed to examine FSH and IGF1 synergy in vivo (19). These mice had normal sex ratios, but exhibited complete female infertility characterized by blockage of early follicle growth. In that model responsiveness to FSH in preantral follicles is lost upon disruption of the IGF signaling pathway. Thus, synergy between FSH and insulin signaling in antral follicles and the potential role of insulin signaling in response to subsequent LH stimulation could not be examined. Several studies indicate that insulin receptor signaling is subject to cross-talk between FSH and LH receptor signaling, through common signaling mediators, that has varying physiological consequences in different stages of follicle growth (6). For example, FSH-dependent activation of the AKT/PI3K pathway in granulosa cells of antral follicles boosts steroidogenesis (20). Whereas, it subsequently stimulates follicular atresia in non-ovulatory follicles (21). Activation of the ERK1/2 pathway in periovulatory follicles is essential for follicular rupture (22) and granulosa/luteal cell differentiation (23). As these signaling pathways also lie downstream of insulin receptor, it suggested the possibility that the early

Author Manuscript Author Manuscript Author Manuscript Author Manuscript

acting *Esr2/Cyp19*-Cre model may have revealed only a portion of insulin's follicular-specific actions in vivo. Indeed, the *Pgr*-Cre driven ablation model employed in this report, escaped the preantral follicle blockage and revealed key contributions of insulin receptor signaling in ovulation, luteal differentiation, and hormone signaling that when disrupted reduce fertility.

Materials and Methods

Mice.

All animal handling was done according to NIH guidelines and in compliance with the Southern Illinois University Carbondale Institutional Animal Care and Use Committee (protocols 16-043, 19-007). Mice used for the study were maintained on a mixed C57BL6 genetic background. All animals were housed under a 12 h light, 12 h dark schedule and fed Purina Labdiet 5008 mouse chow. Genomic DNA was collected from tail snips for genotyping by PCR using the primer sequences shown in Supplemental Table 1. For fertility analyses, vaginal opening was used as the marker for female puberty and female mice were subsequently cycled for 2.5 months prior to breeding trials. We generated mice carrying double floxed alleles for *Insr* and/or *Igf1r* from two previously generated lines where LoxP sites were introduced to flank exons 4 of *Insr* [$Insr^{flox/flox}$, (24)] and exons 3 of *Igf1r* [$Igf1r^{flox/flox}$, (25)]. For conditional tissue-specific ablation, $Insr/Igf1r^{flox/flox}$ mice were bred to male mice expressing the *Pgr-Cre* knock-in allele which has been shown to cause high efficiency ablation of floxed loci in postnatal ovary, uterus, pituitary, and oviduct (26, 27). Specifically in the ovary, *Pgr* is expressed in mural granulosa cells of periovulatory follicles throughout ovulation and in corpora lutea.

Estrous cycle assessment.

Vaginal smears were collected daily for 30 days beginning one week after vaginal opening. Smears were collected at the same time each morning (9 AM) by gently flushing the vagina 3 times with sterile PBS and eluate transferred to glass slides and stained with 0.2% methylene blue to differentiate the proportions of nucleated epithelial cells, cornified squamous epithelial cells, and leukocytes by light microscopy. Stages were classified as follows: Proestrus, primarily nucleated and some cornified cells; Estrus, primarily cornified epithelial cells; Metestrus, cornified epithelial and leukocyte cells; and Diestrus, primarily leukocytes.

Superovulation and hormone assay.

For the superovulation studies, female mice at post-natal day 21-28 (PND21-28), selected by size at least 15 g for maximal response, were treated with 5 IU equine chorionic gonadotropin (eCG, Biovendor RP178272, Asheville, NC). This treatment was followed 48 h later by treatment with 4 IU human chorionic gonadotropin (hCG, Sigma C0434, St. Louis, MO). Both eCG and hCG were dissolved in 0.85 % saline solution and injected i.p. in a total volume of 0.1 ml. Mice were euthanized by CO2 asphyxiation 2-72 h after hCG injection and ovaries and/or oviducts collected for in vitro analyses. One ovary was homogenized in 500 μL of Trizol (Invitrogen) for RNA isolation according to manufacturer's recommendations and the other was fixed in 4 % paraformaldehyde

Author Manuscript Author Manuscript Author Manuscript Author Manuscript

(dissolved in PBS pH 7.4) for 12-16 h, washed with 70% ethanol and stored for later processing. For hormone analyses, blood samples were taken post-mortem by cardiac puncture and serum levels of progesterone (P4, sensitivity 40 ng/ml) determined by ELISA (EIA1561, DRG Diagnostics), and estradiol (E2, sensitivity 3 pg/ml) determined by ELISA (EIA4399, DRG Diagnostics), following the manufacturer's instructions. Oocytes were flushed using a 30G blunt end needle, by injecting PBS pH 7.4 in the oviduct of superovulated females, 12-14h post hCG treatment.

Embryo flushing and assessment of blastocyst quality.

Females were mated with wildtype males overnight, and checked for vaginal plugs in the morning. Three days after observing a vaginal plug [3.5 days post coitum (dpc)] females were sacrificed. The embryos were flushed from the uterine horns using a 27G needle, by injecting PBS pH 7.4 at the utero-tubal junction. Blastocyst quality was analyzed as previously described (28). Briefly, embryos were fixed in 4 % paraformaldehyde (dissolved in PBS pH 7.4) for 20 min, followed by 5ng/mL DAPI staining for 5min. Total cell numbers per blastocyst were counted.

Histological analyses.

Fixed ovaries were embedded in paraffin wax and serial sectioned (5μm) using a microtome. Every 5th serial section was mounted on a glass slide and stained with hematoxylin and eosin for histological evaluation of follicle numbers. Stage of follicular development was assessed using previously defined criteria (29). Briefly, primordial follicles contained an oocyte surrounded by a single layer of squamous granulosa cells, primary follicles contained an oocyte surrounded by a single layer of cuboidal granulosa cells, secondary follicles contained an oocyte surrounded by at least two layers of cuboidal granulosa cells and theca cells, antral follicles contained an oocyte surrounded by multiple layers of cuboidal granulosa cells with a fluid filled antral space and theca cells, and corpora lutea (CL) were much larger structures containing luteal cells. All primordial and primary follicles were counted in each section regardless of nuclear material in the oocyte, whereas only secondary and antral follicles where the oocyte's nucleus was visible were counted to avoid the risk of double counting the larger follicle types that can span multiple sections. Follicles that were comprised of 10% apoptotic bodies were scored as atretic. Follicles transitioning between stages were counted as follicles within the more mature stage of the two stages. The total numbers of all follicles, total numbers of each type of follicle, percentages of each follicle type, and corpora lutea numbers per number of sections counted were recorded. Before staining, ovarian sections were deparaffinated and rehydrated in xylene, 100%, 95%, 70%, and 50% ethanol then PBS. Antigen retrieval using a boiling citrate buffer was performed using an automated Decloaking Chamber (Biocare Medical) as described previously (30). Immunolocalization of proteins was performed in using commercially available primary antibodies at the dilutions shown in Supplemental Table 2. Bound antigens were visualized using biotinylated secondary antibodies and the Vectastain Elite ABC Kit (Vector laboratories, Burlingame, CA). Negative controls were performed in which the primary antibody was substituted with preimmune serum or non-specific serum IgG, as available. Counterstaining with hematoxylin and eosin was performed using standard manufacturer's protocols. The terminal deoxynucleotidyl transferase dUTP nick end labeling (TUNEL)

Author Manuscript Author Manuscript Author Manuscript Author Manuscript

assay was performed according to manufacturer's instructions using ApopTag® Fluorescein In Situ Apoptosis Detection Kit (S7110; Millipore).

Quantitative real-time RT-PCR analysis and RNA-sequencing.

The quantity and quality of total RNA was determined by spectrometry and denaturing agarose gel electrophoresis, respectively. The cDNA was synthesized from total RNA (2 μg) using High-Capacity cDNA Reverse Transcription Kit (Applied Biosystems). Quantitative real-time RT-PCR (qPCR) analysis of mRNA expression was performed as described previously (30, 31), using a CFX96 Real-Time PCR Detection System (BioRad) with Power Up™ SYBR Green Master Mix (Applied Biosystems). Primers (Supplemental Table 3) were designed using NCBI's design tool to span at least one exon/intron junction. Data were normalized against *Rpl19* and are shown as the average fold increase ± standard error of the mean (SEM) with relative expression being calculated using the $2^{-\Delta\Delta CT}$ method as described previously (32). After amplification, the specificity of the PCR was determined by both melt-curve analysis and gel electrophoresis to verify that only a single product of the correct size was present.

For RNA-sequencing analysis, total ovarian RNA was isolated using the RNeasy mini kit (74104, Qiagen) and sent to the Roy J. Carver Biotechnology Center at the University of Illinois for library creation and sequencing as described previously (33). Gene set enrichment analysis (GSEA) was used to identify genetic pathways disrupted by loss of insulin receptor activity as we performed previously (34). The publically available GSEA platform (www.broad.mit.edu) was used with the recommended settings for gene ranking and comparison with gene sets defined as significantly enriched if the FDR q-value was less than 0.2 when using Pearson metrics and 1000 permutations of gene sets. Selected genes of interest were verified by qPCR using RNA samples distinct from those employed for RNA-seq. RNA sequencing data have been deposited in the Gene Expression Omnibus (accession: GSE129222).

Statistics.

For All qPCR, histological measurements, and subfertility analyses data were subjected to one-way ANOVA using Prism 5.0 (GraphPad, San Diego, CA). Comparison of means between two groups were conducted using t test and differences between individual means of multiple grouped data were tested by a Tukey multiple-range test. All data met necessary criteria for ANOVA analysis including equal variance as determined by Bartlett's test. All experimental data are presented as mean ± SEM. Unless otherwise indicated, a P value of 0.05 or less was considered statistically significant.

Results

Conditional knockout of INSR and IGF1R in periovulatory follicles.

In order to determine the essential role of insulin receptor signaling in the ovary without causing severe defects reported in mouse models with a global deficit of INSR or IGF1R (9-11), we generated conditional granulosa cell-specific knockout mice for each receptor (*Insr*-cKO or *Igf1r*-cKO) and mice that lack both *Igf1r* and *Insr* (referred to as IR-cKO

Author Manuscript Author Manuscript Author Manuscript Author Manuscript

hereafter), eliminating the potential for redundancy from receptor cross-talk. Analysis of mRNA expression in whole ovaries from *Insr*-cKO and IR-cKO mice exhibited a significant 45-55% decline in *Insr* levels (Fig. 1A). To the best of our knowledge, INSR protein has not previously been examined in intact ovarian tissues by immunohistochemistry (IHC). In control animals, INSR protein is localized to the granulosa cells of all growing follicles and in most luteal cells (Fig. 1B). In IR-cKO mice, nearly all INSR protein is absent in large antral follicles and corpora lutea, with expression varying in the granulosa layers of preantral follicles (Fig. 1C). Ovarian *Igf1r* expression has been previously characterized and is known to be induced in granulosa cells when follicle growth is initiated and remains highly expressed in periovulatory follicles and in corpora lutea (35). *Igf1r* levels were significantly reduced in both *Igf1r*-cKO and IR-cKO mice (Fig. 1D). The high residual receptor expression in total ovaries from knockout mice is most likely due to the stage-specific ablation elicited by *Pgr*-Cre, as IHC analyses in adult mice that show absent or substantially diminished expression of IGF1R in the granulosa layers of antral and periovulatory follicles, but normal expression in earlier stages (Fig. 1F). Like INSR, the expression of IGF1R was largely absent in corpora lutea of IR-cKO mice.

We hypothesized that as insulin signaling is essential for many cell types to thrive, the loss of one insulin signaling mediator may lead to changes in the relative expression of the other potentially redundant receptor. Studies in epithelial cells and cancer cell lines have demonstrated compensatory upregulation of *Insr* expression and activity upon loss of *Igf1r* (36, 37). The expression of *Igf1r* was equivalent to control levels in *Insr*-cKO mice. Conversely, no changes in *Insr* levels were observed in *Igf1r*-cKO. Thus, for both models, no apparent compensatory upregulation of the other receptor was present in single receptor knockout mice.

Ovarian insulin receptors are essential for female fertility.

Fertility was examined in control, both single knockouts, as well as IR-cKO female cycling mice by mating them with males of proven fertility. As a confirmation of successful mating, we observed vaginal plugs in the controls and all knockout females. While there was an apparent delay for some *Igf1r*-cKO and IR-cKO mice to receive a plug, the duration that was needed for successful mating was not significantly different between groups (Fig. 2A). After the observance of vaginal plugs, male mice were removed and the resulting pregnancy outcomes determined. All control and *Insr*-cKO pairs produced litters, with an average of 7.5 ± 1 pups per litter. However, *Igf1r*-cKO mice exhibited variable litter sizes with an average of 2.25 ± 1 pups per litter (including the 3 females that exhibited no signs of pregnancy) suggesting these single knockouts are subfertile. Ablation of both insulin receptors resulted in complete failure to produce litters from the initial pairing (Fig. 2A).

Subsequently, 4 independent breeding pairs that previously demonstrated ability to mate successfully (evidenced by the presence of vaginal plug 1-2 days after pairing) and produce litters, for genotypes other than IR-cKO, were monitored for 5 months for continuous breeding assessment (Fig. 2B). Control females maintained a consistent monthly litter output of ~7 pups per female. Pup accumulation from *Insr*-cKO females trended lower than controls, but was not significantly different ($P < 0.057$ at 5 months). From the onset, *Igf1r*-

Author Manuscript Author Manuscript Author Manuscript Author Manuscript

cKO mice produced fewer pups per successful pregnancy and often would skip a month between litters leading to significantly lower total pup accumulation. No litters were produced by IR-cKO females in the 5 month trial. In aggregate, when litters are produced, no significant difference in litter size between control and *Insr*-cKO mice was observed (Fig. 2C). However, *Igf1r*-cKO mice produce ~2.5 fewer pups per litter than controls. To date, we have never observed a litter from any IR-cKO females in our colony.

Interestingly, despite their apparent subfertility and/or infertility, no differences in gross ovarian morphology or size were observed in insulin receptor mutant mice. In contrast to other ablation strategies, as insulin-dependent follicle growth was initiated normally in these knockout lines, but failed to produce consistent offspring, our findings suggested that ablation with *Pgr*-Cre represented a unique model to dissect the role of INSR and IGF1R in vivo during ovulation. To rule out potential confounding effects from disruption of insulin signaling upstream of the ovary, including potential pituitary ablation of insulin receptors, we used exogenous gonadotropins to induce superovulation. Histological examination of knockout ovary sections revealed that follicles at all stages of development and corpora lutea were present in control and knockout ovaries, suggesting no significant arrest in folliculogenesis (Fig. 3A). In support of this, serial sectioning of IR-cKO ovaries did not reveal a significantly ($P > 0.5$, n=3) different ratio of follicle counts from that of controls (Fig. 3B). Analysis of follicular atresia revealed no significant differences in follicle health between control (20.25 ± 1.4) and IR-cKO (18.6 ± 1.5) mice (Supplemental Fig. 1A). In addition, no significant differences were found in the number of apoptotic cells within follicles between control and IR-cKO mice as assessed by TUNEL staining (Supplemental Fig. 1B). However, all IR-cKO mice examined to date have shown signs of ovulation failure where corpora lutea (CL) appear to encase trapped oocytes (Fig. 3A, arrows). In the mice employed for follicle counting, 16 of the 28 scored corpora lutea had a trapped oocyte. To examine this further, we superovulated mice collecting them at 12 h post-hCG (shortly after the expected time of ovulation, data not shown) and at 24 h post hCG (when formation of mature corpora lutea should be completed). At both time points we observed trapped oocytes within corpora lutea, suggesting lack of insulin signaling in the periovulatory window results in diminished follicular rupture and release of oocytes as observed in mutants for *Pgr*, *Lhcgr*, *Ptsg2*, and *Efna5* (38-42). In the mice employed for TUNEL analysis, 3 CL contained trapped oocytes. One of these CL contained more TUNEL positive cells than the mean number among corpora lutea from IR-cKO mice, but the other 2 contained only a few apoptotic cells, suggesting that CL death was not a salient feature of oocyte trapping at the stage examined.

To confirm that ovulation was impaired and that oocytes were trapped in luteal tissue and not simply contained in abnormally formed granulosa cell layers, we performed IHC on ovarian sections from superovulated mice at 24 h post-hCG using anti-HSD17B7, a luteal cell marker. Pronounced and uniform staining of luteal cells was present in CL of control animals (Fig. 4A). Differentiation of granulosa cells to luteal cells during corpora lutea formation was observed in IR-cKO mice, as evidenced by HSD17B7 staining, albeit slightly reduced relative to controls. However, the presence of oocytes within luteal tissue was only observed in IR-cKO mice (Fig. 4A, arrow). The expression levels of three genes crucial for ovulation *Lhcgr*, *Pgr* and *Ptgs2* were significantly reduced in these IR-cKO ovaries (Fig.

Author Manuscript Author Manuscript Author Manuscript Author Manuscript

4B). Significant, but less pronounced and more variable reduction of *Lhcgr* and *Ptgs2* was observed in *Igf1r*-null mice. Interestingly, all three lines exhibited similar downregulation of *Pgr*. These data suggest that both receptors are involved in ovulation, acting via potentially distinct downstream targets, and their synergistic function is needed for maximal successful ovulation and subsequent fertility. To assess whether expression of these genes was simply delayed or of misregulation was present throughout follicle growth, we examined relative mRNA expression in additional superovulated mice at 8 h, 12 h, and 24 h post-hCG treatment. *Pgr* and *Ptgs2* were significantly decreased in IR-cKO mice at all 3 time points examined. In contrast, *Lhcgr* was significantly reduced only at 24 h post hCG (Fig. 4C).

The observation of trapped oocytes in luteal tissue, as well as, the reduced expression of genes involved in ovulation led us to hypothesize that ovulation is impaired in IR-cKO mice. To test this, we superovulated female mice, excised their ovaries and oviducts and determined whether oocytes that could potentially be fertilized were being released. In agreement with expected yields from prior studies (43), superovulated control mice released 20-30 oocytes (Fig. 5A). In contrast, oviducts from IR-cKO mice contained significantly fewer (22.6 ± 2.5 vs. 7.7 ± 1.2, $P < 0.001$) exuded oocytes confirming impaired ovulation. As loss of progesterone signaling can elicit impaired ovulation, we attempted to overcome potential progesterone insufficiency by providing supplemental progesterone after superovulation before performing follicle counts or breeding trials. However, this did not increase the number of oocytes that could be flushed from the oviducts of IR-cKO mice, nor did it improve pregnancy outcomes (data not shown).

Since IR-cKO mice are infertile, yet some oocytes are being released, we questioned the competency of IR-cKO oocytes to be fertilized. To test this, we sacrificed normally cycling females bred to males of established fertility at 3.5dpc, excised their uterine horns and examined the presence of blastocyst-stage embryos. In agreement with expected yields (43), control females produced on average 5.83 ± 0.40 blastocysts (Fig. 5B). On the other hand, significantly fewer (1.83 ± 0.5) blastocysts could be flushed from IR-cKO mice. To determine whether these blastocysts were healthy, we assessed the number of cells at this stage of development, an established indicator of embryo quality (28). While control blastocysts contained 51.1 ± 1.5 cells, there were significantly fewer cells (33.2 ± 2.9) present in IR-cKO blastocysts (Fig. 5C). This suggested that blastocyst quality is reduced either do to granulosa cell defects or an oocyte defect. As on indicator of oocyte development, we examined FOXO3, an oocyte-specific Forkhead box protein that is present during primordial and primary stages of folliculogenesis, then is rapidly degraded at the secondary follicle stage upon oocyte activation and maturation (44, 45). In control mice, consistent with expected expression patterns, FOXO3 is detected only in oocytes from both primordial (arrowheads) and primary follicles, and absent from the oocytes of secondary follicles (Fig. 5D). In contrast, while FOXO3 can be detected in the oocytes of primary follicles in IR-cKO mice, it remains prevalent in the majority of oocytes within secondary follicles (Fig. 5E). In control mice, we did not observe any periovulatory follicles that contained FOXO3 positive oocytes. However, FOXO3 stained oocytes surrounded by a cumulus granulosa stalk (*) were frequently observed in IR-cKO ovaries.

Author Manuscript Author Manuscript Author Manuscript Author Manuscript

IR-cKO mice demonstrate misregulation of gene involved in steroidogenesis, lipid metabolism, and TCF3-dependent transcription.

To identify potential granulosa cell factors that contribute to impaired ovulation, we performed RNA-sequencing analysis to identify gene expression differences in IR-cKO mice in the periovulatory window. For this, total ovarian RNA was isolated from superovulated mice 12 h post-hCG (n=4 per genotype). We identified 16,339 expressed sequences, 501 of which were differentially expressed (293 up-regulated, 208 down-regulated) at FDR $P < 0.05$. Gene set enrichment analysis (GSEA) was performed on a ranked list of 245 genes (uncharacterized cDNA were excluded) exhibiting greater than 1.7-fold difference in expression. These misregulated genes primarily exhibited enrichment for metabolic processes including: small molecule metabolic process, lipid metabolic process, metabolism of lipids and lipoproteins, as well as genes responsive to external and endogenous stimulus, and to oxygen containing compound (Supplemental Table 4). The most enriched gene set, CAGGTG_E12_Q6, corresponded to downstream targets of Transcription Factor-3 (TCF3). No specific GO term corresponding to ovulatory processes was significantly enriched, but two corresponding to general reproductive processes, that included *Pgr* and *Lhcgr*, were found among the significant, but less stringent, enriched pathways (Dataset S1).

The prevalence of lipid metabolism factors altered in our RNA-seq, coupled with the significant reduction in *Lhcgr* expression in IR-cKO ovaries (Fig. 4) suggested that diminished expression of both INSR and IGF1R could affect LH-induced steroidogenesis. To test this, we quantified the expression of key genes encoding steroidogenic enzymes in ovaries from superovulated mice at 8 h, 12 h, and 24 h post-hCG. There was significant down-regulation of *Star*, the transport protein responsible for regulating cholesterol distribution in the mitochondria, a rate-limiting step in steroid hormone synthesis (46), and *Cyp11a1*, the enzyme responsible for production of pregnenolone from cholesterol, at both 12 h and 24 h post-hCG (Fig. 6A). The gene encoding the enzyme responsible for subsequent conversion to progesterone, *Hsd3b1*, was significantly upregulated at 8 h when it is involved in the production of estradiol, but subsequently reduced at 24 h, when it is mainly involved in the luteal production of progesterone. Additionally, the luteal cell-specific enzyme *Hsd17b7*, primarily responsible for conversion of estrone to estradiol, but whose ablation leads to reduced serum progesterone (47), was significantly reduced at 24 h post hCG. Similarly to *Hsd3b1*, increased expression of *Cyp19a1* and *Hsd17b1* at 8 h post hCG in IR-cKO was observed (Fig. 6A). No significant misregulation of Cyp17a1, the 17, 20 lyase encoding gene, was observed at any time point examined. Taken together, these changes in gene expression suggested that both granulosa cell and luteal cell hormone production could be compromised. We found that estradiol levels in serum from superovulated IR-cKO mice at 24 h post-hCG was significantly elevated 33% relative to controls (Fig. 6B). We observed serum progesterone levels in superovulated IR-cKO mice which were 2.5-fold lower (16.8 ± 2.7 vs. 6.7 ± 0.9, $P < 0.01$) at 24 h post-hCG and 5-fold lower (24.2 ± 4.5 vs. 5.5 ± 2.4, $P < 0.01$) at 48 h post-hCG compared to controls (Fig. 6C). At 72 h post-hCG, when corpora luteal are quiescent and progesterone production drops in the absence of pregnancy, no significant difference in serum progesterone was observed. The steeper decline in progesterone production between 24 h and 48 h is important because it illustrates that luteal cell differentiation or function is permanently compromised and not

Author Manuscript Author Manuscript Author Manuscript Author Manuscript

simply delayed in developmental time. Normal estrous cyclicity patterns were observed for all female mice in our study, suggesting that hormone signaling upstream of the ovary is intact in our granulosa-specific insulin signaling mutants, and that the elevated estradiol observed in IR-cKO mice is unlikely to be biologically relevant (Fig. 6D).

The role of TCF3 in governing transcription of ovarian cells has not been previously characterized. However, we were able to identify TCF3 targets from the literature that have established or implicated roles in promoting ovarian function. **Note**, this TCF3 is not the same transcription factor associated with β-catenin signaling, which is well-known to regulate ovarian physiology including *Lhcgr* expression (17). That transcription factor is properly termed *Tcf7l1* (www.informatics.jax.org, MGI:1202876), but still appears commonly in the literature as *Tcf3*/TCF3, adding confusion to downstream pathway analyses. The expression differences of selected TCF3-target genes were examined by qPCR analysis of whole ovary tissue (n=6 per genotype) from superovulated mice 12 h post-hCG (Fig. 7). *Scg2*, a potent granulosa cell-specific stimulator of ovarian angiogenesis (48), was down-regulated 5-fold in IR-cKO mice, but not significantly reduced in either *Insr*-cKO or *Igf1r*-cKO ovaries. Significant down-regulation of three membrane-associated transporters was confirmed in IR-cKO mice. The hCG- and PGR-dependent organic anion transporter, *Slco2a1*, contributes to prostaglandin synthesis and action in granulosa cells of ovulatory follicles in humans (49, 50). The zinc transporter, *Slc39a14*, is expressed in cumulus granulosa cells and is thought to regulate free intracellular zinc in mouse oocytes (51). Direct analysis of the amino acid transporter, *Slc7a11*, has primarily been limited to regulation of intracellular glutathione synthesis in neuronal tissue, but could play a similar role in FSH- and LH-dependent glutathione production in granulosa cells to support oocyte health (52-54). Lastly, the expression of *Vcan*, a large chondroitin sulfate proteoglycan component of the extracellular matrix found in many tissues (55), was diminished 6-fold in *Igf1r*-cKO and 10-fold in IR-cKO ovaries.

Reduced activation of Akt by LHCGR in CLs.

As one of the main signaling pathways of both LHCGR and INSR/IGF1R, the AKT/PI3K pathway represents a potential crosslink by which insulin signaling could affect ovulation. Therefore, we examined whether conditional ablation of *Insr* and *Igf1r* would result in diminished AKT1 phosphorylation in ovaries from superovulated IR-cKO mice at 24 h post-hCG. Immunohistochemical analysis with an antibody specific for phospho-Serine473 of AKT1 showed reduced staining in large antral follicles and corpora lutea of IR-cKO mice compared to littermate controls stained under identical conditions (Fig. 8A). This reduction is specific to follicle cells where INSR and IGF1R have been ablated as AKT1 phosphorylation in preantral (primary and secondary) follicles where insulin signaling is still largely intact is not diminished (Fig. 8A).

FOXO1, one of the main targets of AKT signaling in granulosa cells, is expressed in high amounts in granulosa cells of growing follicles, but after FSH and LH stimulation it is pushed out of the nucleus and later degraded in luteal cells (20). This reverse localization is attributed to the ability of FSHR and LHCGR to activate the AKT/PI3K signaling pathway that ultimately leads to the phosphorylation of FOXO1. When we analyzed its localization,

Author Manuscript Author Manuscript Author Manuscript Author Manuscript

while in small antral follicles there was no apparent difference between IR-cKO and controls (Figs. 8B and 8C), in mural granulosa cells of periovulatory follicles in IR-cKO ovaries it appeared to be nuclearly localized compared to the cytoplasmic localization of the controls (Figs. 8D and 8E). This suggests that the activity of INSR and IGF1R is crucial for the activation of the AKT pathway, either directly or in conjunction with LHCGR in mural granulosa and luteal cells.

Discussion

In this study, we conditionally deleted *Insr* and *Igf1r* using *Pgr*-Cre, which led to impaired ovulation, embryo quality, and lutenization culminating in complete infertility when both receptors were absent. We chose to ablate both receptors simultaneously to eliminate potential low affinity cross-interactions of insulin ligands that might mask fertility defects after single ablation of their cognate receptors individual. In contrast to complete insulin receptor knockout lines, IR-cKO mice exhibited no indications of abnormal growth, development, and ability to mate. This was evidenced by normal estrous cycles and the consistent presence of vaginal plugs in pairings of IR-cKO female mice and control males. Prior to our report, studies examining the essential synergy of ovarian insulin signaling and fertility have concentrated on IGF modulation of FSH receptor signaling (19, 56).

To examine the role of IGF signaling in the ovary without the deleterious effects of global IGF or IGF1R knockout (10), Baumgarten et al recently performed conditional ablation of *Igf1r* (19). To achieve complete ablation of IGF1R in granulosa cells, they paired using a combination of *Esr2*-Cre and *Cyp19*-Cre expressing lines and the same $Igf1r^{flox/flox}$ strain used in this study. Mice lacking granulosa IGF1R had smaller ovaries and were completely sterile. Unexpectedly, these mice displayed no difference in FSH receptor levels. However, there was complete arrest of follicle growth at the preantral stage. Granulosa cells that were present failed to differentiate, exhibited premature apoptosis, and ultimately gave rise to follicles that were severely deficient in estrogen production. Treatment with exogenous gonadotropins failed to rescue impaired folliculogenesis indicating the defect was indeed ovary-specific.

We hypothesized that if folliculogenesis was allowed to initiate and continue past this block prior to disruption of insulin signaling, that a heretofore uncharacterized distinct role of insulin signaling during the periovulatory window might be unmasked. As *Pgr*-Cre expression is initiated after that of either *Esr2*-Cre or *Cyp19*-Cre, we found this allowed enough insulin signaling activity to promote follicle growth past the antral stage. The likely critical difference between the models lies in the advanced accumulation of LH responsiveness in *Pgr*-Cre mediated deletion during early antral follicle formation, relative to that of the model used by Stocco's group. However, granulosa cells from eCG-induced *Esr2*-Cre/*Cyp1*9-Cre *Igf1r* conditional knockout mice ($IGF1R^{gcko}$) mice were found to have only a 3-fold reduction in *Lhcgr*, suggesting a decline in receptor expression alone cannot account for the difference (19).

The majority of the fertility defects in our IR-cKO mice come from loss of IGF1R signaling, as *Insr*-cKO mice exhibit nearly normal litter frequencies and litter sizes as compared to

Author Manuscript Author Manuscript Author Manuscript Author Manuscript

control mice. This agrees with findings from INSR^{gcko} mice that exhibited greater variability in average litter size and oocytes ovulated, but no significant differences in diminished mean values compared to controls in a 6-month breeding trial (19). IGF family members can bind INSR (9, 57), but are apparently not required to do so when IGF1R is intact [our work herein, and (19, 58)]. Insulin is commonly added to granulosa cell culture media and has been demonstrated to elicit maximal hormone production in cultured ovarian cells (59-61). These studies and others examining similar mechanisms have often relied on non-physiological effects of INS hormone, so the ratio of relevant INSR vs IGF1R action is difficult to assess when potential cross-reactivity is possible. However, it is clear that INSR-mediated growth and development cannot compensate for the loss of IGF1R activity.

It is possible that during the ovulatory window, there are some unique actions of INSR and IGF1R. We did observe variability in the fertility of *Igf1r*-cKO mice, with a few that exhibit breeding success similar to controls and most producing only 1-2 pups per litter. This finding is similar to that observed when *Esr2*-Cre alone was used to ablate *Igf1r*, where 3-5 pups were produced per litter (19). This difference may be explained by the different time courses of insulin receptor expressions. Our qPCR data show that relative levels of *Insr* and *Igf1r* are consistent during preantral follicle growth. However, just prior to ovulation, there is a decrease in *Igf1r* and increase in *Insr* mRNA levels (data not shown). This suggests that the chance for compensation by INSR might be higher in our model than any of the previous models examining insulin receptor function where ablation occurs earlier. This variability in timing of decreased insulin receptor activity may create different critical thresholds for alteration of downstream activity. This may explain why we see some transcription differences, particularly in the genes known to be essential for ovulation, in single knockout animals vs the IR-cKO mice when putative insulin-regulated genes were examined by qPCR. In addition, this may account for differences in IGF1R-dependent AKT activation, where early termination in IGF1R^{gcko} leads to increased atresia of secondary and antral follicles (19). However, no prematurely induced atresia or significant differences in the number of atretic follicles was seen in our *Pgr*-Cre mediated deletions.

To understand the transcriptome of INSR and IGF1R, we performed RNA-Seq on whole ovaries, 12h post hCG. Not surprisingly, most of the differentially expressed genes were involved in metabolism, as insulin signaling governs energy production and growth processes. This screen confirmed most of our targeted qPCR analyses from 24 h post-hCG superovulated mice and demonstrates that INSR and IGF1R regulate steroidogenesis and PGR signaling even at the onset of ovulation. *Foxo1* mRNA levels were not significantly altered in our RNA-seq, but we did observe that FOXO1 protein was inappropriately nuclearly localized in mural granulosa cells of large antral follicles in IR-cKO mutants. Constitutive activation of nuclear FOXO1 has been shown to inhibit steroid and lipid biosynthetic pathways in granulosa cells, including *Star*, *Cyp11a1*, and *Hsd17b7* that were downregulated in IR-cKO mice (20). Thus, this potential repression could account for many of the changes we observed in IR-cKO superovulated (24 h post-hCG) mice.

An unexpected finding was that the most abundant gene set was CAGGTG_E12_Q6, with a total of 57/245 misregulated genes. This set contains genes which, in their promoter region, contain at least one copy of a TCF3 binding site. To our knowledge, this is the first study to

Author Manuscript Author Manuscript Author Manuscript Author Manuscript

report the presence and potential action of TCF3 in the mouse ovary. Although TCF3, previously known as E2A, has been shown to play a role in lymphopoiesis, where it is required for B and T lymphocyte development (62-66), here we show that it could be involved in ovulation. Previous research has shown that TCF3 activity and expression can be modulated by the Ras-ERK MAPK cascade (67-70), another signaling cascade activated by INSR and IGF1R. The strong downregulation of *Vcan* is potentially relevant to the impaired ovulation and oocyte development observed in IR-cKO mice. VCAN is a proteolytic target of ADAMTS1, matrix metalloprotease that is essential for remodeling of the follicle during ovulation and subsequent vascularization of the CL (71). The anovulatory phenotype observed in progesterone receptor knockout mice is due in part to loss of progesterone-dependent ADAMTS1 cleavage of VCAN (72). Interestingly, *Adamts1* trends down 2-fold in our RNA-seq, but does not reach significance (P >0.057), which may explain why IR-cKO mice are not completely anovulatory. Presumably, the cleavage of VCAN in the extracellular matrix would serve to loosen the associations between cells. Thus, it is surprising that reduced *Vcan* expression would not achieve a similar goal and result in follicle wall destabilization. This suggests that the proteolytic products of VCAN may serve additional roles as signaling molecules within the periovulatory follicle that promote ovulation. In support of this, VCAN contains an epidermal growth factor-like motif whose activity promotes cumulus expansion and oocyte maturation (73). An N-terminal VCAN cleavage peptide, versikine, is thought to modulate cell proliferation and apoptosis, although its mechanism of action is unclear (55). In addition, transcriptome profiling of human cumulus granulosa cells revealed that *VCAN* was positively associated with embryo quality (74), which may contribute to the retarded development we observe in IR-CKO blastocysts. Another putative TCF3-regulated factor of relevance is Secretogranin II (SCG2), which is induced in granulosa cells during the periovulatory window (48). The proteolytic cleavage product of SCG2 (SN peptide) is an established inducer of angiogenesis (75), an essential process for ovulation and CL development and function in rodents and humans (76, 77). SN exhibited a dose-dependent effect on human ovarian endothelial cell sprouting, suggesting it can similarly promote angiogenesis in the ovary (48). SN also serves as a potent chemoattractant for monocytes (78), which are recruited to the CL to promote luteal regression (79). We did not directly assess extension of luteal life span. However, the kinetics of progesterone production and normalcy of ovarian cycles suggest that may not be a significant factor in IR-cKO mice. The putative role of TCF3 in relevant regulation of *Scg2* is complicated as it is known to be regulated by LH (48), and we found that *Lhcgr* is downregulated in IR-cKO ovaries. Thus, additional studies are required to verify the link between TCF3 and insulin signaling, and their intersection with FHS and LH signaling, but we believe TCF3 and its targets represent a potential new piece of the ovulation regulatory network worthy of further investigation.

The disruption in ovulation is not severe enough to resolve the complete infertility of IR-cKO mice. While hormone production is reduced, the hypothalamic-pituitary-gonadal axis elicits normal ovulatory cycles. We found that while fewer oocytes were being released, their fertilization and passage through the oviduct was normal. However, we found two indications that these oocytes may be compromised. First, the persistent presence of FOXO3 in oocytes of antral and periovulatory suggests that the maturation of the oocytes in IR-cKO

Author Manuscript Author Manuscript Author Manuscript Author Manuscript

mice is impaired, likely due to misregulation of some paracrine factors produced by the granulosa cells. Second, following fertilization, the growth of IR-cKO blastocysts lags behind those from control mice. We do not know whether these eventually recover and develop to implantation competency, but no evidence of implantation has been observed. Diminished CL support expected from IR-cKO ovaries would certainly contribute partially to this failure. However, preliminary observations indicate that loss of insulin signaling in progesterone receptor expressing cells of the uterus compromises receptivity. Formal studies to characterize decidualization and embryo implantation in our insulin receptor mutant lines are underway.

In summary, employing a *Pgr-Cre* knock-in model, we successfully ablated ovary-specific insulin signaling after follicle recruitment in the periovulatory window. We demonstrated that insulin actions are necessary for successful oocyte development and ovulation, subsequent blastocyst growth, progesterone synthesis, and fertility. Our findings indicate IGF1R plays a more prominent role in governing overall female fertility than INSR, but the unique phenotype resulting from simultaneous ablation of both receptors in granulosa cells suggests the existence of co-regulated factors and pathways that have yet to be elucidated.

Supplementary Material

Refer to Web version on PubMed Central for supplementary material.

Acknowledgments.

We thank Drs. John Lydon and Francesco DeMayo for the use of *Pgr*-Cre mice. We also thank Dr. Buffy Ellsworth for providing the anti-FOXO1, and anti-FOXO3 antibodies. We acknowledge the Southern Illinois University Histology Core Facility and director Stacey McGee for sample embedding.

Support: These studies were supported by a Research Seed Grant from the Southern Illinois University School of Medicine and by Eunice Kennedy Shriver National Institute of Child Health and Human Development Grant HD093802.

Nonstandard Abbreviations:

CGC	cumulus granulosa cell
cKO	conditional knockout
CL	corpus luteum
eCG	equine chorionic gonadotropin
E2	estradiol
FSH	follicle-stimulating hormone
GC	granulosa cell
hCG	human chorionic gonadotropin
IGFBP	insulin-like growth factor binding protein

Author Manuscript Author Manuscript Author Manuscript Author Manuscript

IHC	immunohistochemistry
LH	luteinizing hormone
MGC	mural granulosa cell
P4	progesterone
qPCR	quantitative real-time RT-PCR
WT	wild type

References

1. Boucher J, Kleinridders A, and Kahn CR (2014) Insulin receptor signaling in normal and insulin-resistant states. Cold Spring Harb Perspect Biol 6
2. Dupont J, and LeRoith D (2001) Insulin and insulin-like growth factor I receptors: similarities and differences in signal transduction. Horm Res 55 Suppl 2, 22–26 [PubMed: 11684871]
3. Benyoucef S, Surinya KH, Hadaschik D, and Siddle K (2007) Characterization of insulin/IGF hybrid receptors: contributions of the insulin receptor L2 and Fn1 domains and the alternatively spliced exon 11 sequence to ligand binding and receptor activation. The Biochemical journal 403, 603–613 [PubMed: 17291192]
4. Belfiore A, Frasca F, Pandini G, Sciacca L, and Vigneri R (2009) Insulin receptor isoforms and insulin receptor/insulin-like growth factor receptor hybrids in physiology and disease. Endocrine reviews 30, 586–623 [PubMed: 19752219]
5. Haywood NJ, Slater TA, Matthews CJ, and Wheatcroft SB (2019) The insulin like growth factor and binding protein family: Novel therapeutic targets in obesity & diabetes. Mol Metab 19, 86–96 [PubMed: 30392760]
6. Dupont J, and Scaramuzzi RJ (2016) Insulin signalling and glucose transport in the ovary and ovarian function during the ovarian cycle. The Biochemical journal 473, 1483–1501 [PubMed: 27234585]
7. Baumgarten SC, Convissar SM, Fierro MA, Winston NJ, Scoccia B, and Stocco C (2014) IGF1R signaling is necessary for FSH-induced activation of AKT and differentiation of human Cumulus granulosa cells. The Journal of clinical endocrinology and metabolism 99, 2995–3004 [PubMed: 24848710]
8. Zhou P, Baumgarten SC, Wu Y, Bennett J, Winston N, Hirshfeld-Cytron J, and Stocco C (2013) IGF-I signaling is essential for FSH stimulation of AKT and steroidogenic genes in granulosa cells. Molecular endocrinology 27, 511–523 [PubMed: 23340251]
9. Accili D, Drago J, Lee EJ, Johnson MD, Cool MH, Salvatore P, Asico LD, Jose PA, Taylor SI, and Westphal H (1996) Early neonatal death in mice homozygous for a null allele of the insulin receptor gene. Nat Genet 12, 106–109 [PubMed: 8528241]
10. Liu JP, Baker J, Perkins AS, Robertson EJ, and Efstratiadis A (1993) Mice carrying null mutations of the genes encoding insulin-like growth factor I (Igf-1) and type 1 IGF receptor (Igf1r). Cell 75, 59–72 [PubMed: 8402901]
11. Louvi A, Accili D, and Efstratiadis A (1997) Growth-promoting interaction of IGF-II with the insulin receptor during mouse embryonic development. Developmental biology 189, 33–48 [PubMed: 9281335]
12. Pitetti JL, Torre D, Conne B, Papaioannou MD, Cederroth CR, Xuan S, Kahn R, Parada LF, Vassalli JD, Efstratiadis A, and Nef S (2009) Insulin receptor and IGF1R are not required for oocyte growth, differentiation, and maturation in mice. Sex Dev 3, 264–272 [PubMed: 19851056]
13. Pitetti JL, Calvel P, Romero Y, Conne B, Truong V, Papaioannou MD, Schaad O, Docquier M, Herrera PL, Wilhelm D, and Nef S (2013) Insulin and IGF1 receptors are essential for XX and XY gonadal differentiation and adrenal development in mice. PLoS genetics 9, e1003160 [PubMed: 23300479]

Author Manuscript Author Manuscript Author Manuscript Author Manuscript

14. Kim J, Bagchi IC, and Bagchi MK (2009) Control of ovulation in mice by progesterone receptor-regulated gene networks. Molecular human reproduction 15, 821–828 [PubMed: 19815644]
15. Richards JS, and Ascoli M (2018) Endocrine, Paracrine, and Autocrine Signaling Pathways That Regulate Ovulation. Trends Endocrinol Metab 29, 313–325 [PubMed: 29602523]
16. Adashi EY, Resnick CE, D'Ercole AJ, Svoboda ME, and Van Wyk JJ (1985) Insulin-like growth factors as intraovarian regulators of granulosa cell growth and function. Endocrine reviews 6, 400–420 [PubMed: 2992919]
17. Law NC, Weck J, Kyriss B, Nilson JH, and Hunzicker-Dunn M (2013) Lhcgr expression in granulosa cells: roles for PKA-phosphorylated beta-catenin, TCF3, and FOXO1. Molecular endocrinology 27, 1295–1310 [PubMed: 23754802]
18. Mani AM, Fenwick MA, Cheng Z, Sharma MK, Singh D, and Wathes DC (2010) IGF1 induces up-regulation of steroidogenic and apoptotic regulatory genes via activation of phosphatidylinositol-dependent kinase/AKT in bovine granulosa cells. Reproduction 139, 139–151 [PubMed: 19819918]
19. Baumgarten SC, Armouti M, Ko C, and Stocco C (2017) IGF1R Expression in Ovarian Granulosa Cells Is Essential for Steroidogenesis, Follicle Survival, and Fertility in Female Mice. Endocrinology 158, 2309–2318 [PubMed: 28407051]
20. Liu Z, Rudd MD, Hernandez-Gonzalez I, Gonzalez-Robayna I, Fan HY, Zeleznik AJ, and Richards JS (2009) FSH and FOXO1 regulate genes in the sterol/steroid and lipid biosynthetic pathways in granulosa cells. Molecular endocrinology 23, 649–661 [PubMed: 19196834]
21. Fan HY, Liu Z, Cahill N, and Richards JS (2008) Targeted disruption of Pten in ovarian granulosa cells enhances ovulation and extends the life span of luteal cells. Molecular endocrinology 22, 2128–2140 [PubMed: 18606860]
22. Fan HY, Liu Z, Shimada M, Sterneck E, Johnson PF, Hedrick SM, and Richards JS (2009) MAPK3/1 (ERK1/2) in ovarian granulosa cells are essential for female fertility. Science 324, 938–941 [PubMed: 19443782]
23. Wayne CM, Fan HY, Cheng X, and Richards JS (2007) Follicle-stimulating hormone induces multiple signaling cascades: evidence that activation of Rous sarcoma oncogene, RAS, and the epidermal growth factor receptor are critical for granulosa cell differentiation. Molecular endocrinology 21, 1940–1957 [PubMed: 17536007]
24. Bruning JC, Michael MD, Winnay JN, Hayashi T, Horsch D, Accili D, Goodyear LJ, and Kahn CR (1998) A muscle-specific insulin receptor knockout exhibits features of the metabolic syndrome of NIDDM without altering glucose tolerance. Mol Cell 2, 559–569 [PubMed: 9844629]
25. Dietrich P, Dragatsis I, Xuan S, Zeitlin S, and Efstratiadis A (2000) Conditional mutagenesis in mice with heat shock promoter-driven cre transgenes. Mammalian genome : official journal of the International Mammalian Genome Society 11, 196–205 [PubMed: 10723724]
26. Peng J, Monsivais D, You R, Zhong H, Pangas SA, and Matzuk MM (2015) Uterine activin receptor-like kinase 5 is crucial for blastocyst implantation and placental development. Proceedings of the National Academy of Sciences of the United States of America 112, E5098–5107 [PubMed: 26305969]
27. Soyal SM, Mukherjee A, Lee KY, Li J, Li H, DeMayo FJ, and Lydon JP (2005) Cre-mediated recombination in cell lineages that express the progesterone receptor. Genesis 41, 58–66 [PubMed: 15682389]
28. Pan Y, Wang M, Wang L, Xu G, Baloch AR, Kashif J, Fan J, and Yu S (2019) Interleukin-1 beta induces autophagy of mouse preimplantation embryos and improves blastocyst quality. Journal of cellular biochemistry
29. Hannon PR, Niermann S, and Flaws JA (2016) Acute Exposure to Di(2-Ethylhexyl) Phthalate in Adulthood Causes Adverse Reproductive Outcomes Later in Life and Accelerates Reproductive Aging in Female Mice. Toxicol Sci 150, 97–108 [PubMed: 26678702]
30. Brown RM, Davis MG, Hayashi K, and MacLean JA (2013) Regulated expression of Rhox8 in the mouse ovary: evidence for the role of progesterone and RHOX5 in granulosa cells. Biology of reproduction 88, 126 [PubMed: 23536368]
31. Welborn JP, Davis MG, Ebers SD, Stodden GR, Hayashi K, Cheatwood JL, Rao MK, and MacLean JA 2nd. (2015) Rhox8 Ablation in the Sertoli Cells Using a Tissue-Specific RNAi

Author Manuscript Author Manuscript Author Manuscript Author Manuscript

Approach Results in Impaired Male Fertility in Mice. Biology of reproduction 93, 8 [PubMed: 25972016]

32. Livak KJ, and Schmittgen TD (2001) Analysis of relative gene expression data using real-time quantitative PCR and the 2(-Delta Delta C(T)) Method. Methods 25, 402–408 [PubMed: 11846609]
33. Prather GR, MacLean JA 2nd, Shi M, Boadu DK, Paquet M, and Hayashi K (2016) Niclosamide As a Potential Nonsteroidal Therapy for Endometriosis That Preserves Reproductive Function in an Experimental Mouse Model. Biology of reproduction 95, 76 [PubMed: 27535961]
34. Stodden GR, Lindberg ME, King ML, Paquet M, MacLean JA, Mann JL, DeMayo FJ, Lydon JP, and Hayashi K (2015) Loss of Cdh1 and Trp53 in the uterus induces chronic inflammation with modification of tumor microenvironment. Oncogene 34, 2471–2482 [PubMed: 24998851]
35. Bassuk AG, Barton KP, Anandappa RT, Lu MM, and Leiden JM (1998) Expression pattern of the Ets-related transcription factor Elf-1. Mol Med 4, 392–401 [PubMed: 10780882]
36. Titone R, Zhu M, and Robertson DM (2018) Insulin mediates de novo nuclear accumulation of the IGF-1/insulin Hybrid Receptor in corneal epithelial cells. Sci Rep 8, 4378 [PubMed: 29531349]
37. Zhang H, Pelzer AM, Kiang DT, and Yee D (2007) Down-regulation of type I insulin-like growth factor receptor increases sensitivity of breast cancer cells to insulin. Cancer research 67, 391–397 [PubMed: 17210722]
38. Buensuceso AV, Son AI, Zhou R, Paquet M, Withers BM, and Deroo BJ (2016) Ephrin-A5 Is Required for Optimal Fertility and a Complete Ovulatory Response to Gonadotropins in the Female Mouse. Endocrinology 157, 942–955 [PubMed: 26672804]
39. Davis BJ, Lennard DE, Lee CA, Tiano HF, Morham SG, Wetsel WC, and Langenbach R (1999) Anovulation in cyclooxygenase-2-deficient mice is restored by prostaglandin E2 and interleukin-1beta. Endocrinology 140, 2685–2695 [PubMed: 10342859]
40. Morham SG, Langenbach R, Loftin CD, Tiano HF, Vouloumanos N, Jennette JC, Mahler JF, Kluckman KD, Ledford A, Lee CA, and Smithies O (1995) Prostaglandin synthase 2 gene disruption causes severe renal pathology in the mouse. Cell 83, 473–482 [PubMed: 8521477]
41. Lei ZM, Mishra S, Zou W, Xu B, Foltz M, Li X, and Rao CV (2001) Targeted disruption of luteinizing hormone/human chorionic gonadotropin receptor gene. Molecular endocrinology 15, 184–200 [PubMed: 11145749]
42. Lydon JP, DeMayo FJ, Funk CR, Mani SK, Hughes AR, Montgomery CA Jr., Shyamala G, Conneely OM, and O'Malley BW (1995) Mice lacking progesterone receptor exhibit pleiotropic reproductive abnormalities. Genes & development 9, 2266–2278 [PubMed: 7557380]
43. Luo C, Zuniga J, Edison E, Palla S, Dong W, and Parker-Thornburg J (2011) Superovulation strategies for 6 commonly used mouse strains. J Am Assoc Lab Anim Sci 50, 471–478 [PubMed: 21838974]
44. John GB, Gallardo TD, Shirley LJ, and Castrillon DH (2008) Foxo3 is a PI3K-dependent molecular switch controlling the initiation of oocyte growth. Developmental biology 321, 197–204 [PubMed: 18601916]
45. John GB, Shirley LJ, Gallardo TD, and Castrillon DH (2007) Specificity of the requirement for Foxo3 in primordial follicle activation. Reproduction 133, 855–863 [PubMed: 17616716]
46. Caron KM, Soo SC, Wetsel WC, Stocco DM, Clark BJ, and Parker KL (1997) Targeted disruption of the mouse gene encoding steroidogenic acute regulatory protein provides insights into congenital lipoid adrenal hyperplasia. Proceedings of the National Academy of Sciences of the United States of America 94, 11540–11545 [PubMed: 9326645]
47. Jokela H, Rantakari P, Lamminen T, Strauss L, Ola R, Mutka AL, Gylling H, Miettinen T, Pakarinen P, Sainio K, and Poutanen M (2010) Hydroxysteroid (17beta) dehydrogenase 7 activity is essential for fetal de novo cholesterol synthesis and for neuroectodermal survival and cardiovascular differentiation in early mouse embryos. Endocrinology 151, 1884–1892 [PubMed: 20185768]
48. Hannon PR, Duffy DM, Rosewell KL, Brannstrom M, Akin JW, and Curry TE Jr. (2018) Ovulatory Induction of SCG2 in Human, Nonhuman Primate, and Rodent Granulosa Cells Stimulates Ovarian Angiogenesis. Endocrinology 159, 2447–2458 [PubMed: 29648638]

Author Manuscript Author Manuscript Author Manuscript Author Manuscript

49. Choi Y, Rosewell KL, Brannstrom M, Akin JW, Curry TE Jr., and Jo M (2018) FOS, a Critical Downstream Mediator of PGR and EGF Signaling Necessary for Ovulatory Prostaglandins in the Human Ovary. The Journal of clinical endocrinology and metabolism 103, 4241–4252 [PubMed: 30124866]
50. Choi Y, Wilson K, Hannon PR, Rosewell KL, Brannstrom M, Akin JW, Curry TE Jr., and Jo M (2017) Coordinated Regulation Among Progesterone, Prostaglandins, and EGF-Like Factors in Human Ovulatory Follicles. The Journal of clinical endocrinology and metabolism 102, 1971–1982 [PubMed: 28323945]
51. Lisle RS, Anthony K, Randall MA, and Diaz FJ (2013) Oocyte-cumulus cell interactions regulate free intracellular zinc in mouse oocytes. Reproduction 145, 381–390 [PubMed: 23404848]
52. Abazari-Kia AH, Mohammadi-Sangcheshmeh A, Dehghani-Mohammadabadi M, Jamshidi-Adegani F, Veshkini A, Zhandi M, Cinar MU, and Salehi M (2014) Intracellular glutathione content, developmental competence and expression of apoptosis-related genes associated with G6PDH-activity in goat oocyte. Journal of assisted reproduction and genetics 31, 313–321 [PubMed: 24356867]
53. Hoang YD, Nakamura BN, and Luderer U (2009) Follicle-stimulating hormone and estradiol interact to stimulate glutathione synthesis in rat ovarian follicles and granulosa cells. Biology of reproduction 81, 636–646 [PubMed: 19516019]
54. Lim J, Nakamura BN, Mohar I, Kavanagh TJ, and Luderer U (2015) Glutamate Cysteine Ligase Modifier Subunit (Gclm) Null Mice Have Increased Ovarian Oxidative Stress and Accelerated Age-Related Ovarian Failure. Endocrinology 156, 3329–3343 [PubMed: 26083875]
55. Nandadasa S, Foulcer S, and Apte SS (2014) The multiple, complex roles of versican and its proteolytic turnover by ADAMTS proteases during embryogenesis. Matrix Biol 35, 34–41 [PubMed: 24444773]
56. Zhou J, Kumar TR, Matzuk MM, and Bondy C (1997) Insulin-like growth factor I regulates gonadotropin responsiveness in the murine ovary. Molecular endocrinology 11, 1924–1933 [PubMed: 9415397]
57. Siddle K (2012) Molecular basis of signaling specificity of insulin and IGF receptors: neglected corners and recent advances. Front Endocrinol (Lausanne) 3, 34 [PubMed: 22649417]
58. Nandi A, Wang X, Accili D, and Wolgemuth DJ (2010) The effect of insulin signaling on female reproductive function independent of adiposity and hyperglycemia. Endocrinology 151, 1863–1871 [PubMed: 20176725]
59. Krasnow JS, Hickey GJ, and Richards JS (1990) Regulation of aromatase mRNA and estradiol biosynthesis in rat ovarian granulosa and luteal cells by prolactin. Molecular endocrinology 4, 13–12 [PubMed: 1970119]
60. Munir I, Yen HW, Geller DH, Torbati D, Bierden RM, Weitsman SR, Agarwal SK, and Magoffin DA (2004) Insulin augmentation of 17alpha-hydroxylase activity is mediated by phosphatidyl inositol 3-kinase but not extracellular signal-regulated kinase-1/2 in human ovarian theca cells. Endocrinology 145, 175–183 [PubMed: 14512432]
61. Zhang G, Garmey JC, and Veldhuis JD (2000) Interactive stimulation by luteinizing hormone and insulin of the steroidogenic acute regulatory (StAR) protein and 17alpha-hydroxylase/17,20-lyase (CYP17) genes in porcine theca cells. Endocrinology 141, 2735–2742 [PubMed: 10919257]
62. Bhalla S, Spaulding C, Brumbaugh RL, Zagort DE, Massari ME, Murre C, and Kee BL (2008) differential roles for the E2A activation domains in B lymphocytes and macrophages. J Immunol 180, 1694–1703 [PubMed: 18209066]
63. de Pooter RF, and Kee BL (2010) E proteins and the regulation of early lymphocyte development. Immunol Rev 238, 93–109 [PubMed: 20969587]
64. King AM, Keating P, Prabhu A, Blomberg BB, and Riley RL (2009) NK cells in the CD19− B220+ bone marrow fraction are increased in senescence and reduce E2A and surrogate light chain proteins in B cell precursors. Mech Ageing Dev 130, 384–392 [PubMed: 19428458]
65. Kwon K, Hutter C, Sun Q, Bilic I, Cobaleda C, Malin S, and Busslinger M (2008) Instructive role of the transcription factor E2A in early B lymphopoiesis and germinal center B cell development. Immunity 28, 751–762 [PubMed: 18538592]

Author Manuscript Author Manuscript Author Manuscript Author Manuscript

66. Lin YC, Jhunjhunwala S, Benner C, Heinz S, Welinder E, Mansson R, Sigvardsson M, Hagman J, Espinoza CA, Dutkowski J, Ideker T, Glass CK, and Murre C (2010) A global network of transcription factors, involving E2A, EBF1 and Foxo1, that orchestrates B cell fate. Nat Immunol 11, 635–643 [PubMed: 20543837]

67. Bain G, Cravatt CB, Loomans C, Alberola-Ila J, Hedrick SM, and Murre C (2001) Regulation of the helix-loop-helix proteins, E2A and Id3, by the Ras-ERK MAPK cascade. Nat Immunol 2, 165–171 [PubMed: 11175815]

68. Li R, Li Y, Hu X, Lian H, Wang L, and Fu H (2016) Transcription factor 3 controls cell proliferation and migration in glioblastoma multiforme cell lines. Biochem Cell Biol 94, 247–255 [PubMed: 27105323]

69. Neufeld B, Grosse-Wilde A, Hoffmeyer A, Jordan BW, Chen P, Dinev D, Ludwig S, and Rapp UR (2000) Serine/Threonine kinases 3pK and MAPK-activated protein kinase 2 interact with the basic helix-loop-helix transcription factor E47 and repress its transcriptional activity. The Journal of biological chemistry 275, 20239–20242 [PubMed: 10781029]

70. Segales J, Islam AB, Kumar R, Liu QC, Sousa-Victor P, Dilworth FJ, Ballestar E, Perdiguero E, and Munoz-Canoves P (2016) Chromatin-wide and transcriptome profiling integration uncovers p38alpha MAPK as a global regulator of skeletal muscle differentiation. Skelet Muscle 6, 9 [PubMed: 26981231]

71. Brown HM, Dunning KR, Robker RL, Boerboom D, Pritchard M, Lane M, and Russell DL (2010) ADAMTS1 cleavage of versican mediates essential structural remodeling of the ovarian follicle and cumulus-oocyte matrix during ovulation in mice. Biology of reproduction 83, 549–557 [PubMed: 20592310]

72. Russell DL, Doyle KM, Ochsner SA, Sandy JD, and Richards JS (2003) Processing and localization of ADAMTS-1 and proteolytic cleavage of versican during cumulus matrix expansion and ovulation. The Journal of biological chemistry 278, 42330–42339 [PubMed: 12907688]

73. Dunning KR, Watson LN, Zhang VJ, Brown HM, Kaczmarek AK, Robker RL, and Russell DL (2015) Activation of Mouse Cumulus-Oocyte Complex Maturation In Vitro Through EGF-Like Activity of Versican. Biology of reproduction 92, 116 [PubMed: 25810476]

74. Liu Q, Zhang J, Wen H, Feng Y, Zhang X, Xiang H, Cao Y, Tong X, Ji Y, and Xue Z (2018) Analyzing the Transcriptome Profile of Human Cumulus Cells Related to Embryo Quality via RNA Sequencing. Biomed Res Int 2018, 9846274 [PubMed: 30155486]

75. Kirchmair R, Egger M, Walter DH, Eisterer W, Niederwanger A, Woell E, Nagl M, Pedrini M, Murayama T, Frauscher S, Hanley A, Silver M, Brodmann M, Sturm W, Fischer-Colbrie R, Losordo DW, Patsch JR, and Schratzberger P (2004) Secretoneurin, an angiogenic neuropeptide, induces postnatal vasculogenesis. Circulation 110, 1121–1127 [PubMed: 15326074]

76. Richards JS, Russell DL, Ochsner S, and Espey LL (2002) Ovulation: new dimensions and new regulators of the inflammatory-like response. Annual review of physiology 64, 69–92

77. Stouffer RL, Xu F, and Duffy DM (2007) Molecular control of ovulation and luteinization in the primate follicle. Front Biosci 12, 297–307 [PubMed: 17127300]

78. Kong C, Gill BM, Rahimpour R, Xu L, Feldman RD, Xiao Q, McDonald TJ, Taupenot L, Mahata SK, Singh B, O'Connor DT, and Kelvin DJ (1998) Secretoneurin and chemoattractant receptor interactions. J Neuroimmunol 88, 91–98 [PubMed: 9688329]

79. Walusimbi SS, and Pate JL (2013) Physiology and Endocrinology Symposium: role of immune cells in the corpus luteum. Journal of animal science 91, 1650–1659 [PubMed: 23422006]

Author Manuscript
Author Manuscript
Author Manuscript
Author Manuscript

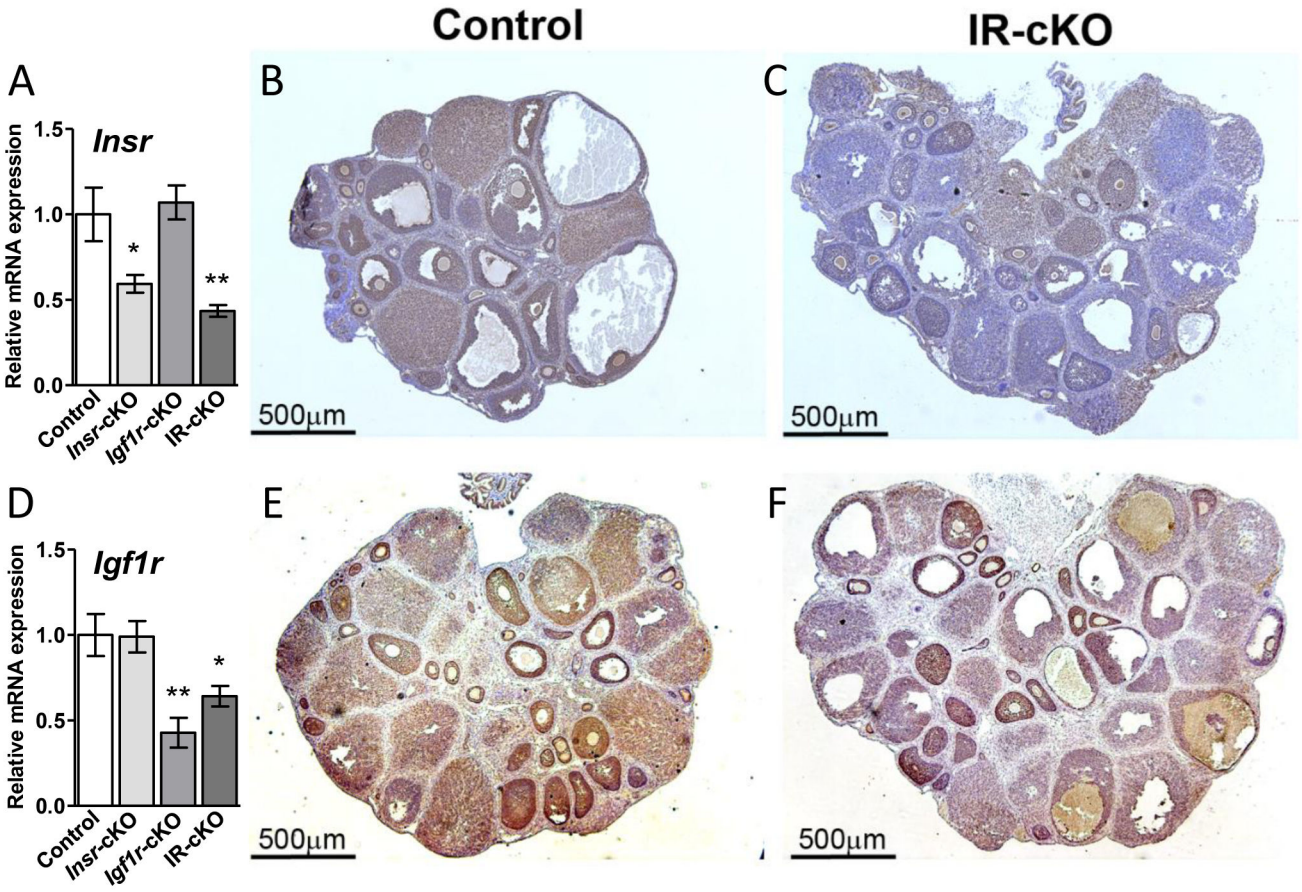

Figure 1.

Conditional ablation of *Insr* and *Igf1r* using *Pgr*-Cre reduces receptor expression in antral follicles and corpora lutea. Samples are from superovulated mice 24 h post-hCG. (*A*) *Insr* expression is significantly reduced in total ovarian mRNA from *Insr*-cKO and IR-cKO mice as assessed by qPCR. Data are expressed as mean ± SEM (n=5, **P* <0.05, ***P* <0.01). (*B*) Immunohistochemistry (IHC) shows cytoplasmic localization of INSR in granulosa cells of growing follicles and luteal cells of corpora lutea (CL). (*C*) IHC showing expression of INSR is markedly decreased specifically in the granulosa cell layer of antral follicles and in the CL after conditional ablation of *Insr*. (*D*) *Igf1r* expression is significantly reduced (n=5, **P* <0.05, ***P* <0.01) in total ovarian mRNA from *Igf1r*-cKO and IR-cKO mice as assessed by qPCR. (*E*) IHC shows abundant cytoplasmic localization of IGF1R in granulosa cells of growing follicles and in CL. (*F*) IHC showing expression of IGF1R is markedly decreased specifically in the granulosa cell layer of antral follicles and in the CL after conditional ablation of *Insr*. IHC images show a representative result obtained in 4 biological repeats.

Author Manuscript
Author Manuscript
Author Manuscript
Author Manuscript

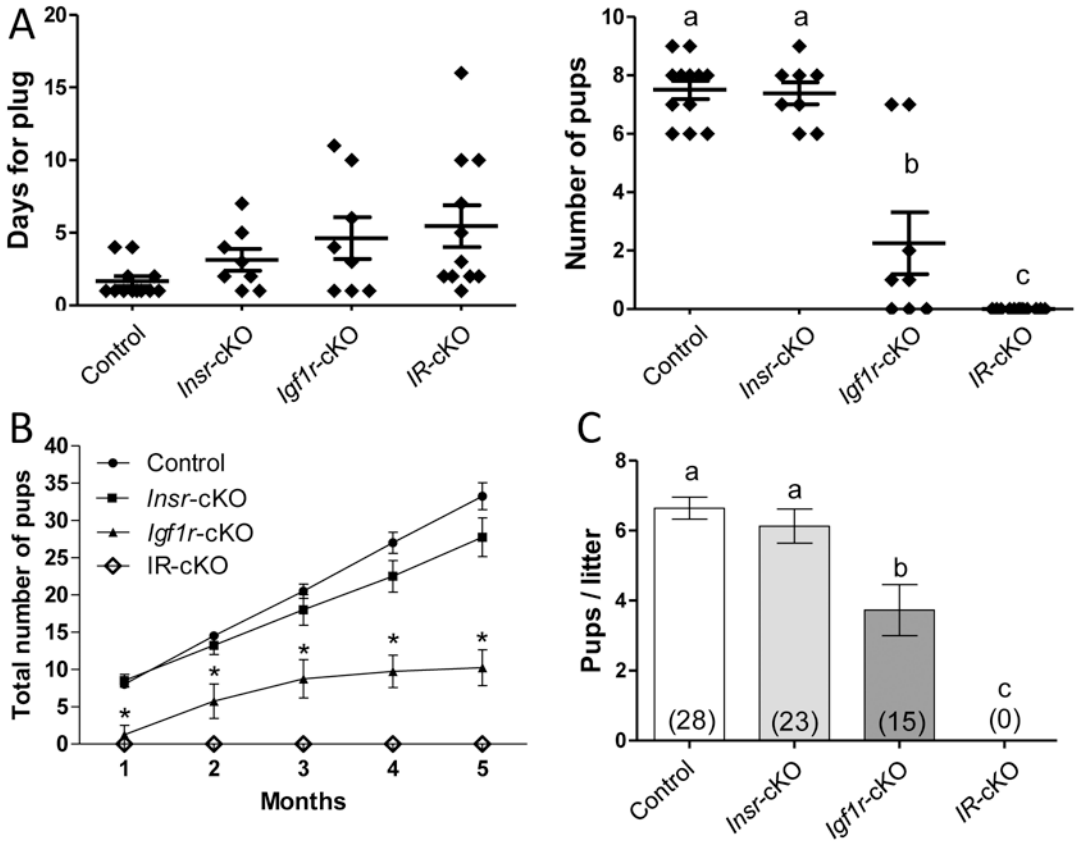

Figure 2.

Female IR-cKO mice are infertile. (*A*) Females from control (n=12), each single receptor knockout (n=8), and double receptor knockout (n=12) groups were bred to males of established fertility. All mice presented with vaginal plugs indicating mating had occurred. The apparent delay to receive the plug in *Insr*-cKO, *Igf1r*-cKO, and IR-cKO mice was not significantly different than controls. After the observation of a vaginal plug, males were separated and females monitored for subsequent pregnancy and parturition. Litter sizes in *Insr*-cKO were not significantly different from control pairs. In contrast, *Igf1r*-cKO exhibited significant subfertility and IR-cKO mice failed to produce any litters. Letters denote means that are significantly different, $P < 0.05$. *(B)* Two month old females of established fertility (for control and single receptor knockout groups) and 4 randomly selected IR-cKO females were paired with males of established fertility and monitored for 5 months. Continuous breeding assessment shows cumulative number of progeny per female (n=4, $*P < 0.001$). *(C)* Aggregate pups per litter among pairings that produced a litter. Total number of litters indicated in each column. Letters denote means that are significantly different, $P < 0.05$.

Author Manuscript
Author Manuscript
Author Manuscript
Author Manuscript

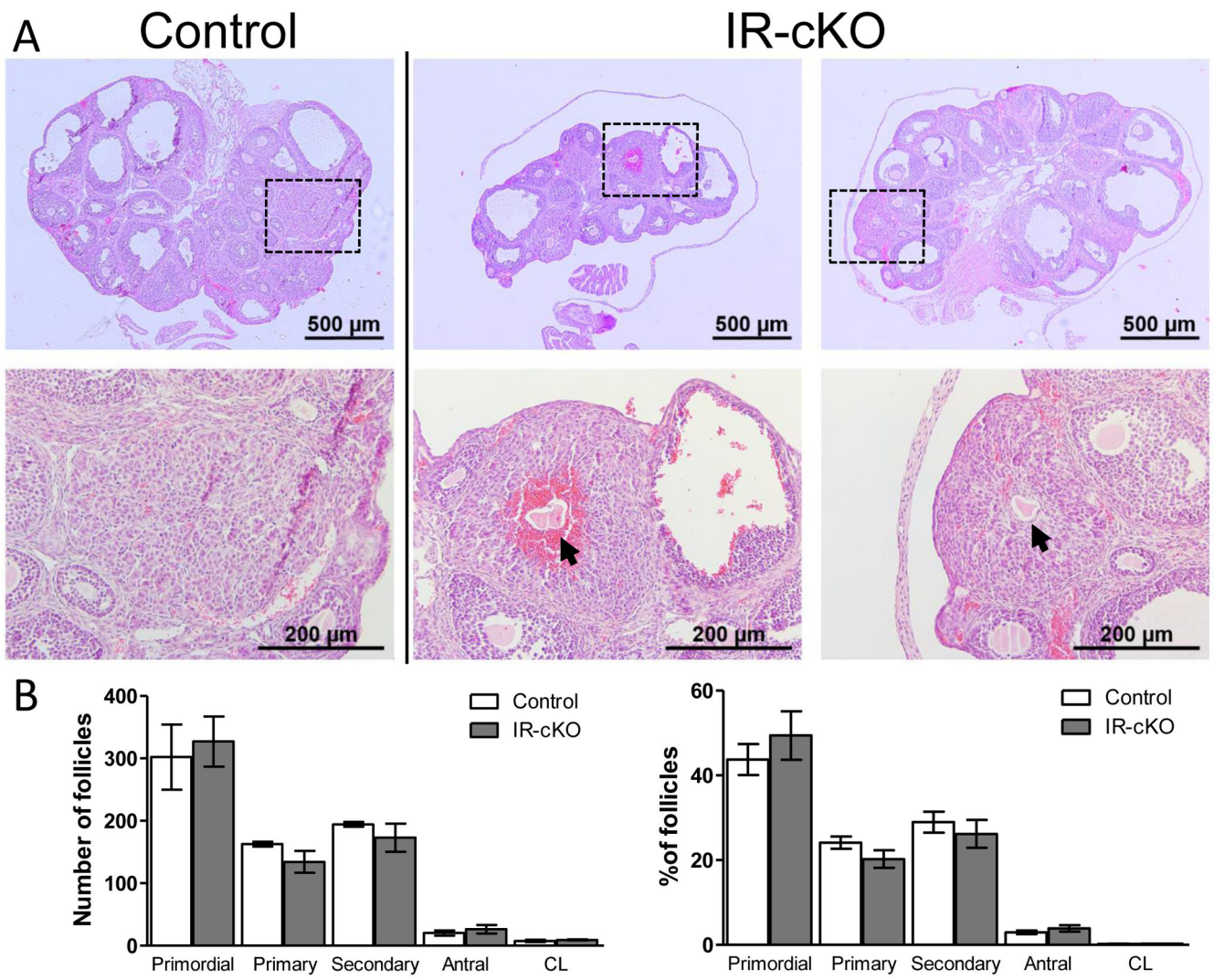

Figure 3.

Histological analysis of IR-cKO ovaries reveals impaired ovulation. Samples are from superovulated mice 24 h post-hCG. *(A)* Gross analysis of ovarian morphology of IR-cKO mice (2 representative animals) exhibits no decrease in ovarian size. However, all animals exhibit signs of anovulation characterized by oocytes trapped in putative CL tissue (arrows). Boxes indicate the region illustrated by the higher magnification panel below each image. *(B)* Ovarian follicle distribution is not significantly different in IR-cKO mice compared to controls. Complete ovaries were serially sectioned and numbers of each follicle type scored. Data are presented as mean ± SEM (n=3).

Author Manuscript Author Manuscript Author Manuscript Author Manuscript

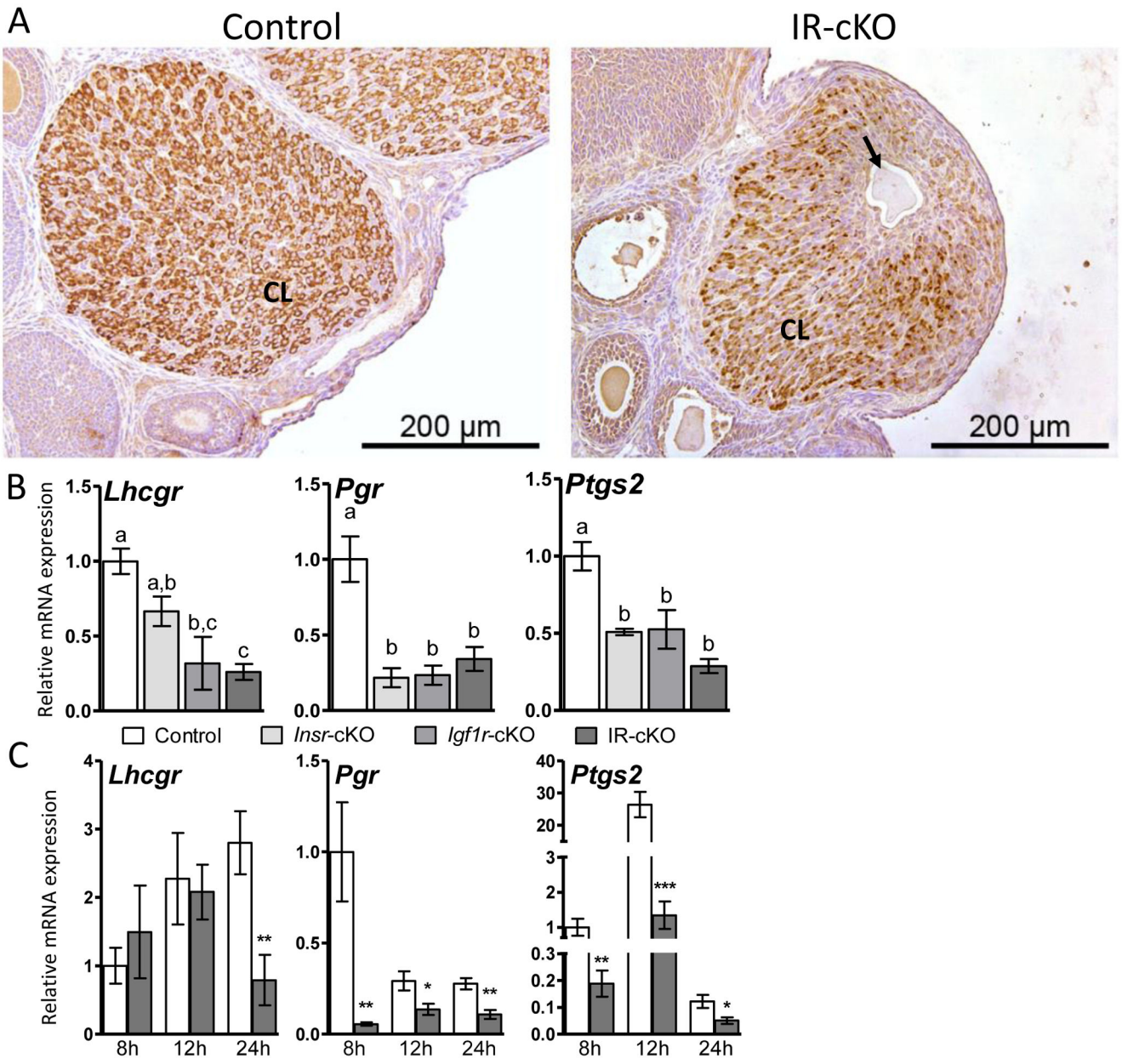

Figure 4.

Ovulation is impaired in IR-cKO mice. Mice were superovulated and sacrificed at 24 h post-hCG when ovulation should be completed and well-formed CL present. (*A*) IHC of the luteal marker HSD17B7 confirms a trapped oocyte (arrow) residing in CL tissue and not the granulosa cell layer of large follicles. (*B*) qPCR showing essential ovulation genes are downregulated in total ovarian mRNA from insulin receptor knockout mice [n=10 (control and IR-cKO) and n=5 (*Insr*-cKO and *Igf1r*-cKO)] at 24 h post-hCG. Data is presented as mean ± SEM fold expression compared to control which was arbitrarily set to 1. Letters denote means that are significantly different $P<0.05$. (*C*) To assess the temporal expression pattern of these markers, five additional females per genotype were superovulated and sacrificed at 8 h, 12 h, and 24 h post-hCG. Relative mRNA expression is presented as mean

± SEM. qPCR of five independent control and IR-cKO females was normalized to control 8 h post-hCG, which was arbitrarily set to baseline of 1 (* $P < 0.05$, ** $P < 0.01$, ** $P < 0.001$ vs. Control).

Author Manuscript Author Manuscript Author Manuscript Author Manuscript

Author Manuscript Author Manuscript Author Manuscript Author Manuscript

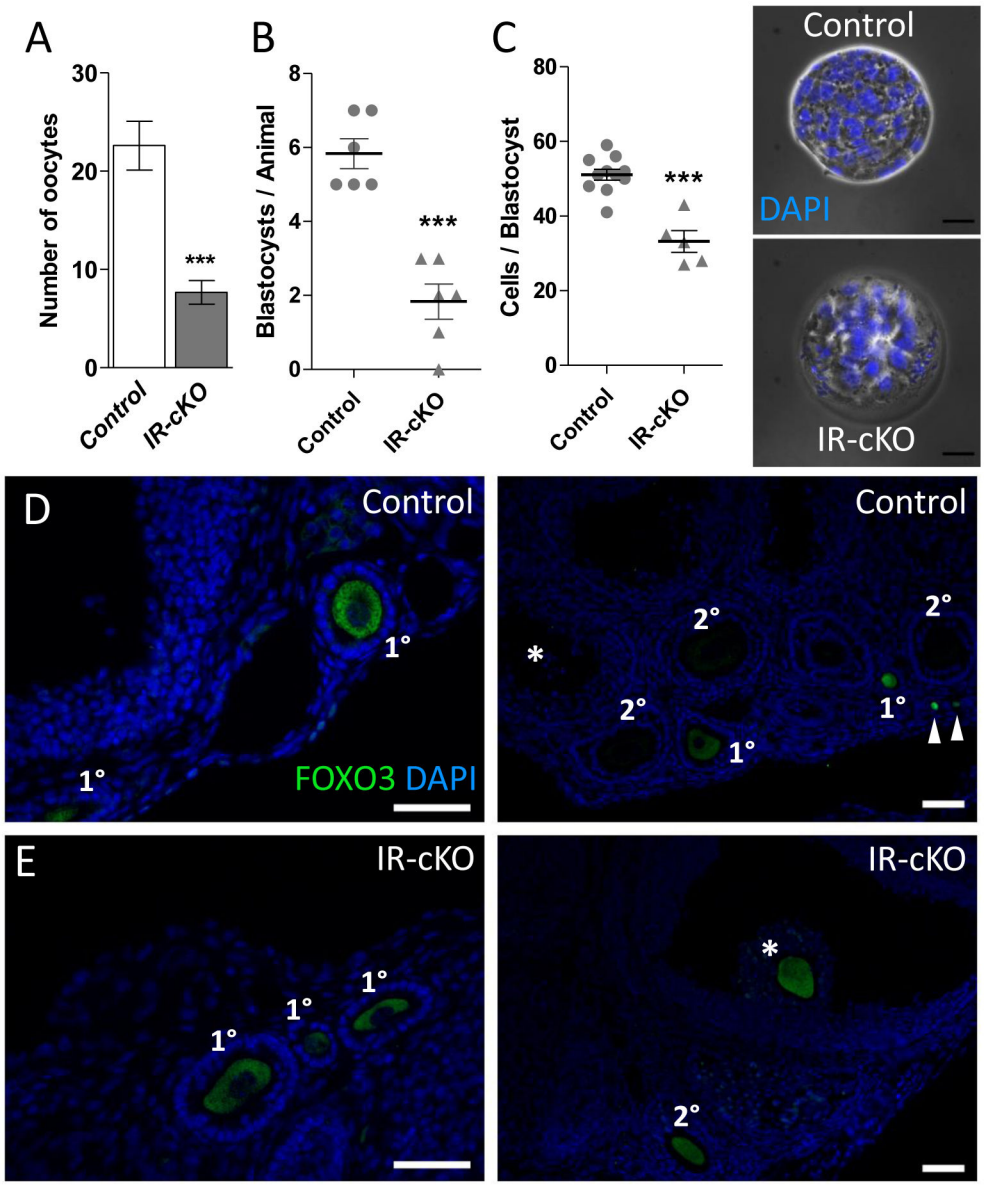

Figure 5. Abnormal ovulation and oocyte/embryo development in IR-cKO mice.

(*A*) Control and IR-cKO mice were superovulated and their oviducts retrieved and flushed 12-14 h post-hCG. Significantly fewer oocytes were retrieved from oviducts of superovulated IR-cKO mice compared to control females (n=6, $P<0.001$). (*B*) Normal cycling females were bred with males of established fertility and their uteri flushed 3.5 days post coitum (dpc). Significantly fewer blastocysts were retrieved from IR-cKO females (n=6, $P<0.001$). (*C*) To assess embryo quality, cell nuclei were stained with DAPI and the number of cells per blastocyst was scored. Scale bar = 25 μm. (*D and E*) Representative images from immunolocalization of FOXO3 protein in oocytes of control (*D*) and IR-cKO (*E*) superovulated mice 24 h post-hCG (n = 3 per genotype, scale bars = 100 μm. FOXO3 is present in primordial (arrowheads) and primary follicles, but absent in secondary and antral (*) follicles of control mice. As expected FOXO3 is found in the oocytes of early stage

primary follicles (left panel) in IR-cKO mice. However, in IR-cKO the presence of FOXO3 is maintained in secondary and periovulatory (*) follicles.

Author Manuscript Author Manuscript Author Manuscript Author Manuscript

Author Manuscript Author Manuscript Author Manuscript Author Manuscript

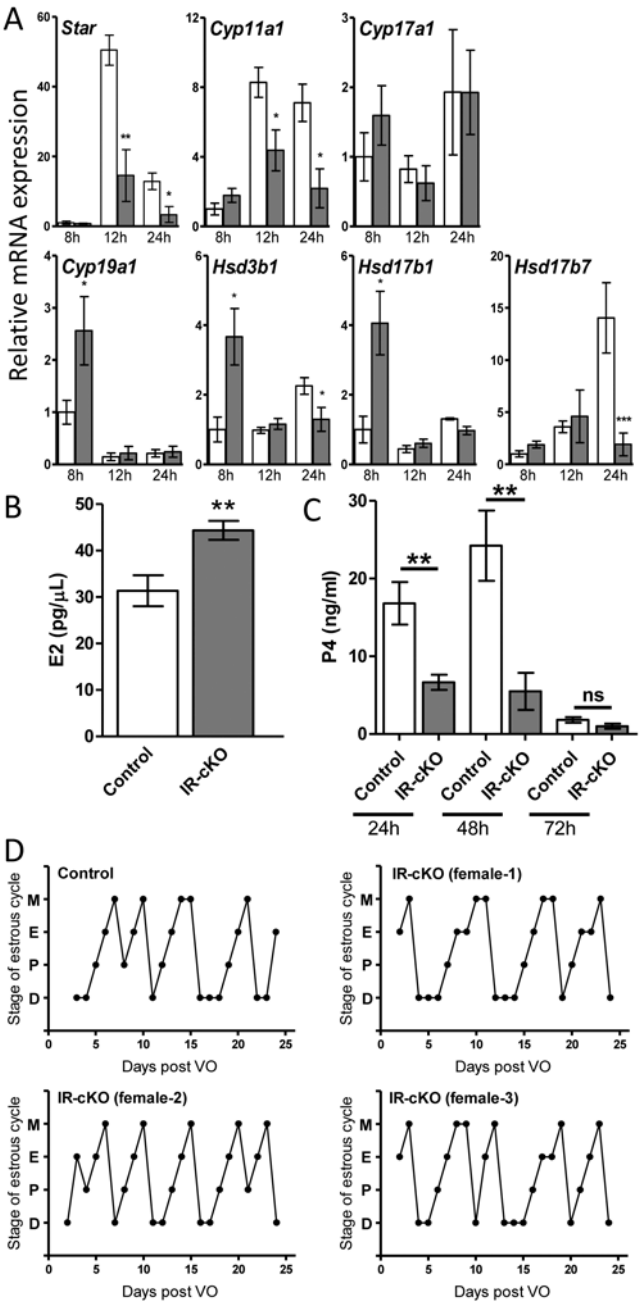

Figure 6.

Steroid synthesis genes are misregulated in mice lacking insulin receptors. (*A*) Relative gene expression was determined by qPCR in total ovary mRNA from superovulated mice (n=6 per time point) at 8 h, 12 h, and 24 h post-hCG. Relative mRNA expression is presented as mean ± SEM. qPCR of five independent control and IR-cKO females was normalized to control 8 h post-hCG, which was arbitrarily set to baseline of 1 (* $P < 0.05$, ** $P < 0.01$, ** $P < 0.001$ vs. Control). (*B*) Serum levels of estradiol are significantly higher in superovulated IR-cKO mice at 24 h post-hCG (n=8, ** $P < 0.01$). (*C*) Serum levels of progesterone are significantly lower in superovulated IR-cKO mice at 24 h post-hCG and 48

Author Manuscript Author Manuscript Author Manuscript Author Manuscript

h post-hCG (n=8, $^{**}P<0.01$). *(D)* Changes in hormone levels do not disrupt estrous cyclicity in IR-cKO mice. Patterns for a representative control and 3 representative IR-cKO female mice are shown. Time in each stage is shown, M-metestrus, E-estrus, P-proestrus, D-diestrus, as defined in the methods.

Author Manuscript Author Manuscript Author Manuscript Author Manuscript

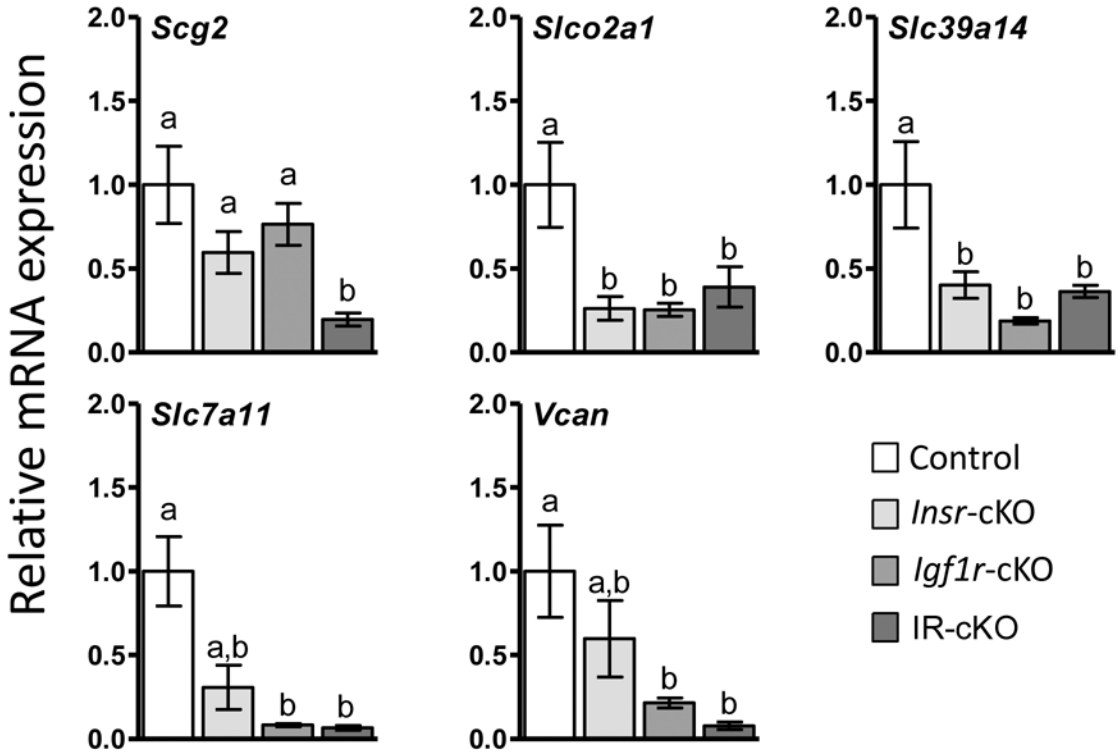

Figure 7.
qPCR verification of selected TCF3-regulated genes misregulated in 12 h post-hCG superovulated IR-cKO mice identified by RNA-seq (n=5 per genotype).

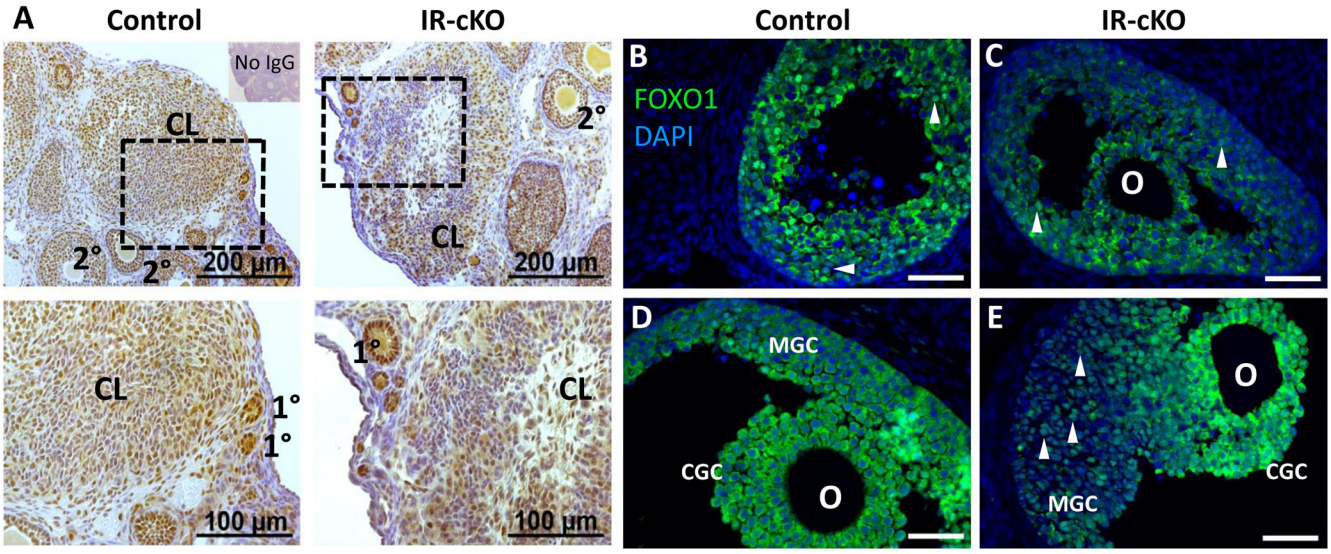

Figure 8.

Insulin receptor signaling mediator AKT1 exhibits reduced phosphorylation in IR-cKO mice. Samples are from superovulated mice 24 h post-hCG. (*A*) IHC showing diminished phosphorylation of Ser473, a residue of AKT1 activated by insulin receptor stimulation, in a representative animal from each genotype (n=3). Dashed boxes indicate the location of the higher magnification images in the lower panels. Reduced phosphor-AKT1 correlates to large antral follicles and CL where insulin receptors were ablated by *Pgr*-Cre expression (see Fig. 1) and not globally impaired as primary and secondary follicles retain normal AKT1 activation. (*B-E*) Immunolocalization of FOXO1, an AKT1-dependent target, is altered in IR-cKO mice. In early antral follicles (*B and C*), FOXO1 exhibits either nuclear or cytoplasmic localization, present only in granulosa cells, and it does not seem affected by the INSR and IGF1R knockout. (*D*) In periovulatory follicles of control mice, FOXO1 is translocated to the cytoplasm of both mural granulosa cells (MGC) and cumulus granulosa cells (CGC). (*E*) However, while the localization of FOXO1 in IR-cKO seems not to be altered in CGC, it is nuclearly localized in MGCs. Arrowheads denote cells with nuclear localization of FOXO1; O-oocyte.

Author Manuscript Author Manuscript Author Manuscript Author Manuscript